Impact of 7,8-Dihydro-8-oxoguanine on Methylation of the CpG Site by Dnmt3a[†]

Diana V. Maltseva,[‡] Alexander A. Baykov,[‡] Albert Jeltsch,[§] and Elizaveta S. Gromova*[,‡]

Chemistry Department and A. N. Belozersky Institute of Physico-Chemical Biology, Moscow State University, Moscow 119991, Russia, and Biochemistry Laboratory, School of Engineering and Science, Jacobs University Bremen, Campus Ring 1, 28759 Bremen, Germany

ABSTRACT: 7,8-Dihydro-8-oxoguanine (8-oxoG) is a ubiquitous oxidative DNA lesion resulting from injury to DNA via reactive oxygen species. 8-oxoG lesions may play a role in the formation of aberrant DNA methylation patterns during carcinogenesis. In this study, we assessed the effects of 8-oxoG on methylation and complex formation of nine 30-mer oligodeoxynucleotide duplexes by the catalytic domain of murine Dnmt3a DNA methyltransferase (Dnmt3a-CD). The effects of 8-oxoG on the methylation rate of hemimethylated duplexes varied from a 25-fold decrease to a 1.8-fold increase, depending on the position of the lesion relative to the Dnmt3a-CD recognition site (<u>C</u>pG) and target cytosine (<u>C</u>). The most significant effect was observed when 8-oxoG replaced guanine within the recognition site immediately downstream of the target cytosine. Fluorescence polarization experiments with fluorescein-labeled duplexes revealed that two molecules of Dnmt3a-CD bind per duplex, generating sigmoid binding curves. Duplexes exhibiting the highest apparent binding cooperativity formed the least stable 1:2 complexes with Dnmt3a-CD and were methylated at the lowest rate. Kinetic analyses disclosed the formation of very stable nonproductive enzyme−substrate complexes with hemimethylated duplexes that act as suicide substrates of Dnmt3a-CD. The presence of 8-oxoG within the <u>C</u>pG site downstream of the target cytosine markedly diminished productive versus nonproductive binding. We propose that 8-oxoG located adjacent to the target cytosine interferes with methylation by weakening the affinity of DNA for Dnmt3a-CD, thereby favoring a nonproductive binding mode.

DNA is constantly attacked by reactive oxygen species generated during normal cellular metabolism and exposure to ionizing or ultraviolet radiation (*1−3*). Guanine is the most readily oxidized of the four heterocyclic bases (*4, 5*). One of the major base lesions is 7,8-dihydro-8-oxoguanine (8-oxoG)[1] (*6*). Replacement of guanine with 8-oxoG does not severely alter the DNA structure, as both bases form three similar hydrogen bonds with cytosine (*7, 8*). However, local distortion of helical parameters around the damaged guanine is evident (*6*). In double-stranded DNA, the native *anti* conformation of the oxidized 2′-deoxyguanosine residue is maintained, but in cases where DNA is single-stranded, such as the replication or transcription stage, the 8-oxoG analogue favors the *syn* conformation (*2, 6, 9*). Consequently, 8-oxoG lesions lead to the loss of base pairing specificity (*3*). While mammalian cells contain OGG1 DNA glycosylase, which removes 8-oxoG opposite cytosine (*2*), unrepaired DNA lesions accumulate with time and contribute to the development of age-related diseases (*3, 5*). An elevated level of oxidative damage has additionally been noted in several tumors (*2*). Thus, 8-oxoG is a biomarker of oxidative stress and, potentially, carcinogenesis (*3, 10*).

8-oxoG can influence the interactions of DNA with different proteins. For instance, 8-oxoG decreases the strand cleavage activity of human topoisomerase I but enhances DNA binding (*11, 12*). These effects are explained by assuming that direct contact of the 8-oxoG oxygen atom, O8, with topoisomerase I stabilizes it as an inactive conformation (*12*). The presence of 8-oxoG in promoter elements of genes prevents binding of the transcription factors, AP1 and SP1 (*13, 14*). Moreover, this lesion inhibits the initial binding of methyl-CpG-binding proteins *in vivo*, interfering with subsequent steps in the chromatin condensation cascade and resulting in potentially heritable epigenetic alterations (*15*). It is hypothesized that oxidative damage of DNA leads to cancer, not only due to the mutagenic effects of such lesions but also due to the epigenetic changes in chromatin organization and gene expression (*3, 10, 16*).

DNA methylation is an important epigenetic mechanism involved in the regulation of gene expression and parental imprinting. In mammalian DNA, methylation occurs at CpG sites and is performed by C5 cytosine DNA methyltransferases (MTases) comprising Dnmt1 specific for hemimethylated DNA and two *de novo* MTases, Dnmt3a and Dnmt3b (*17, 18*). Aberration of DNA methylation is closely associated with various chronic diseases, including cancer and diabetes (*19, 20*). Replacement of guanine with 8-oxoG profoundly diminishes the ability of Dnmt1 to methylate its

[1] Abbreviations: AdoHcy, *S*-adenosyl-L-homocysteine; AdoMet, *S*-adenosyl-L-methionine; Dnmt3a-CD, catalytic domain of the DNA methyltransferase Dnmt3a; MTase, DNA methyltransferase; FAM, 6(5)-carboxyfluorescein; 8-oxoG, 7,8-dihydro-8-oxoguanine.

Table 1: Oligodeoxynucleotide Sequences[a]

designation	sequence
GCGC (or GCGCTC)	5′-CTGAATACTACTTGCGCTCTCTAACCTGAT
GMGC	5′-CTGAATACTACTTGMGCTCTCTAACCTGAT
CGCG	5′-ATCAGGTTAGAGAGCGCAAGTAGTATTCAG
CGMG	5′-ATCAGGTTAGAGAGMGCAAGTAGTATTCAG
fGCGC (or fGCGCTC)	5′-FAM-CTGAATACTACTTGCGCTCTCTAACCTGAT
CGMGf	5′-FAM-ATCAGGTTAGAGAGMGCAAGTAGTATTCAG
XCGC	5′-CTGAATACTACTTXCGCTCTCTAACCTGAT
GCXC	5′-CTGAATACTACTTGCXCTCTCTAACCTGAT
CGMX	5′-ATCAGGTTAGAGAXMGCAAGTAGTATTCAG
CXMG	5′-ATCAGGTTAGAGAGMXCAAGTAGTATTCAG
CGMGAX	5′-ATCAGGTTAGAXAGMGCAAGTAGTATTCAG

[a] M, 5-methylcytosine; X, 8-oxoG; FAM, 6-carboxyfluorescein.

target cytosine, suggesting that damage leads to the formation of aberrant DNA methylation patterns (*16, 21*). Moreover, substitution of either of the guanines of the CCGG recognition site of prokaryotic MTase HpaII with 8-oxoG dramatically alters enzyme binding to DNA and inhibits methylation (*22*).

The purpose of this study was to establish the effects of oxidative damage in DNA on methylation by Dnmt3a. Our results show that 8-oxoG significantly suppresses the methylation activity of the catalytic domain of Dnmt3a (Dnmt3a-CD) by stimulating the formation of tight nonproductive complexes with DNA.

EXPERIMENTAL PROCEDURES

Chemicals. AdoHcy was purchased from Sigma (St. Louis, MO). [CH_3-^{3}H]AdoMet (77 Ci/mmol, 13 μM) was obtained from Amersham Biosciences (Little Chalf-ont, U.K.). All oligodeoxynucleotides (Table 1) were purchased from Syntol (Moscow, Russia). The fluorescein label (FAM) was introduced at the 5′-end of the oligodeoxynucleotides by means of an aminoalkyl linker containing six methylene groups. Oligodeoxynucleotides were purified by polyacrylamide gel electrophoresis and eluted as a single band by the manufacturer. The oligodeoxynucleotide concentrations were estimated spectrophotometrically (*23*).

The following buffers (A–G) were used: A, 20 mM KH_2PO_4-KOH (pH 7.5), 500 mM NaCl, 10 mM β-mercaptoethanol, 10% (v/v) glycerol, 0.1% Triton X-100, and 20 mM imidazole-HCl; B, buffer A containing 40 mM imidazole-HCl; C, buffer A containing 200 mM imidazole-HCl; D, 20 mM HEPES-NaOH (pH 7.5), 100 mM KCl, 1 mM EDTA, 0.2 mM dithiothreitol; E, buffer D containing 10% (v/v) glycerol; F, buffer D containing 50% (v/v) glycerol; and G, 10 mM Tris-HCl (pH 7.9), 50 mM NaCl, 1 mM dithiothreitol, and 0.1 mg/mL acetylated BSA.

Enzyme Expression and Purification. The N-terminal His_6 tag fusion catalytic domain of Dnmt3a was expressed in BL21(DE3) *Escherichia coli* cells using pET28a containing Dnmt3a-CD as the vector, as described previously (*24*). Protein expression was initiated at a cell density corresponding to an A_{600} of 0.5 by the addition of 1 mM IPTG. After 4 h, cells were harvested by centrifugation and disrupted with an MSE Sonifier (Crawley, U.K.) in buffer A. Protein purification was performed in the presence of a protein inhibitor cocktail (Roche), as recommended by the supplier. Cell debris was removed by centrifugation (30 min at 13000 rpm). The supernatant was applied to a Co-Talon metal

affinity resin column (BD Biosciences Clontech) equilibrated with buffer A. After being washed with buffers A and B, Dnmt3a-CD was eluted with buffer C. The eluate was dialyzed overnight against buffer E and for 2 h against buffer F. The final preparation of Dnmt3a-CD was >90% pure, as assessed by electrophoresis on a 12.5% polyacrylamide gel in the presence of 0.1% sodium dodecyl sulfate. The Dnmt3a-CD concentration was determined by Bradford analysis and expressed as a monomer concentration.

Expression of N-terminal His_6 tag fusion M.SssI and determination of the active enzyme concentration were performed as described in a previous report (*25*).

Methylation Assay. DNA methylation by Dnmt3a-CD was monitored by measuring the amount of tritium incorporated into the oligodeoxynucleotide duplexes in buffer D at 37 °C (*26, 27*). Two types of single-turnover experiments were conducted. In the first set of measurements, the substrate concentration used was a 1.7-fold molar excess over Dnmt3a-CD, but only a small proportion was converted due to low catalytic activity of the enzyme. The concentrations of the oligodeoxynucleotide duplexes, Dnmt3a-CD, and [CH_3-^{3}H]AdoMet were 1.5, 0.88, and 2 μM, respectively. After 1–15 min, aliquots of the reaction mixtures were pipetted onto DE-81 paper disks (Whatman, Berntford, U.K.) and treated as described previously (*27*). The rates (*v*) of methylation for all oligodeoxynucleotide duplexes were determined from the initial linear regions of the product (methylated DNA) versus time profiles.

In the second set of measurements, the reaction mixtures contained 300 nM oligodeoxynucleotide, 3 μM Dnmt3a-CD, and 1.2 μM [CH_3-^{3}H]AdoMet (i.e., enzyme concentration 10-fold greater than that of the substrate). The reaction was allowed to proceed for 4–90 min to completion. The rate constant of methylation under single-turnover conditions (k_{st}) was estimated with eq 1, where [MS] and [MS]$_f$ represent the concentrations of methylated DNA at time *t* and the end point of the reaction, respectively:

$$[MS] = [MS]_f(1 - e^{-k_{st}t}) \qquad (1)$$

The kinetics of methylation by M.SssI were measured in buffer G containing 500 nM oligodeoxynucleotide duplex, 20 nM M.SssI, and 1.2 μM [CH_3-^{3}H]AdoMet. Aliquots of the reaction mixtures were withdrawn after 1–3.5 min and analyzed as described above for Dnmt3a-CD.

Fluorescence Polarization Measurements. Fluorescence polarization by the FAM-labeled oligodeoxynucleotide duplexes was measured at 25 °C in 120 μL of buffer D using a Cary Eclipse fluorimeter (Varian) with excitation at 495 nm and emission at 520 nm. Fluorescence polarization (*P*) was defined in terms of the vertical (I_v) and horizontal (I_h) emission components as $P = (I_v - GI_h)/(I_v + I_h)$, where *G* is the instrumental correction factor. Oligodeoxynucleotide duplexes (10 nM) containing the FAM label in one of the DNA strands were preincubated with 0.1 mM AdoHcy, and fluorescence polarization by free DNA (P_0) was measured. Dnmt3a-CD was added as 0.5–4 μL aliquots of a 3 μM stock solution at a final concentration of 300–560 nM, and the polarization value (*P*) was recorded 2 min after each addition. To reduce the concentration of glycerol added with enzyme to the assay medium, the stock enzyme solution was prepared by diluting its more concentrated solution in buffer F 3.7-

fold with buffer D. Control experiments disclosed a negligible effect of glycerol at the highest concentration (2.5%) used in the assay medium. Each titration curve was obtained in at least triplicate.

Binding data were analyzed in terms of Scheme 1:

Scheme 1

$$E \xrightarrow{K_{d1}} ES \xrightarrow{K_{d2}} E_2S$$
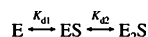
where E represents homodimeric Dnmt3a-CD, S is FAM-labeled DNA, and ES and E_2S are the complexes. The dissociation constants, K_{d1} and K_{d2}, were obtained by simultaneously fitting eqs 2−6 to the dependences of the measured polarization values, P, on total Dnmt3a-CD concentration, $[E]_0$, with SCIENTIST from MacroMath (St. Louis, MO).

$$P = P_0 + (P_{max} - P_0)(0.5[ES] + [E_2S])/[S]_0 \quad (2)$$

$$[E][S]/[ES] = K_{d1} \quad (3)$$

$$[E][ES]/[E_2S] = K_{d2} \quad (4)$$

$$[E] + [ES] + 2[E_2S] = [E]_0 \quad (5)$$

$$[S] + [ES] + [E_2S] = [S]_0 \quad (6)$$

P_0 and P_{max} are the fluorescence polarization values for free and fully bound DNA, respectively, while $[S]$ and $[S]_0$ represent free total DNA concentrations. This treatment takes into account the decrease in free DNA and free enzyme concentrations due to complex formation. Equation 2 assumes that the contribution of E_2S to the fluorescence polarization value is twice that for ES, as E_2 is approximately twice as great in volume as E. Equations 3 and 4 define the binding constants, while eqs 5 and 6 describe mass conservation for Dnmt3a-CD and DNA, respectively.

RESULTS

To elucidate the effects of 7,8-dihydro-8-oxoguanine lesions (X) on the ability of Dnmt3a-CD to methylate DNA, we prepared ten 30-mer oligodeoxynucleotide duplexes and assessed their binding to and/or methylation by Dnmt3a-CD. 8-oxoG lesions were incorporated into one strand of the hemimethylated and unmethylated DNA duplexes within the Dnmt3a-CD recognition sequence (GCXC/CGMG, GCGC/CXMG, and GCXC/CGCG), adjacent to it on the 5′-side (XCGC/CGMG, GCGC/CGMX, and XCGC/CGCG), or distant from the site (GCGCTC/CGMGAX) (Table 2). Hemimethylated substrates contained m5dC instead of target dC in the neighborhood of 8-oxoG (GCGC/CXMG, GCGC/CGMX, and GCGCTC/CGMGAX) or the complementary strand (GCXC/CGMG and XCGC/CGMG) (Table 2).

The melting curves of unmethylated XCGC/CGCG and GCXC/CGCG containing 8-oxoG were cooperative (data not shown) with melting temperatures ranging from 64.4 to 66.5 °C, which were 1.3 °C lower and 0.5 °C higher than that of the unmodified GCGC/CGCG duplex, respectively. Therefore, 8-oxoG lesions have an only minor effect on the stability of 30-mer duplexes.

Initial Rates of Methylation by Dnmt3a-CD. The kinetic parameters of 8-oxoG-damaged oligodeoxynucleotide duplex methylation by Dnmt3a-CD were measured under conditions where the DNA concentration was 1.7-fold greater than that of enzyme. The time courses were linear in all cases for

hemimethylated duplexes, as illustrated in Figure 1. The relative methylation rates, v^{rel}, are presented in Table 2. A 25-fold decrease in v^{rel} was observed for the hemimethylated duplex, GCXC/CGMG, containing 8-oxoG within the CpG site. In contrast, methylation of the GCGC/CXMG duplex containing 8-oxoG opposite the target dC was faster by a factor of 1.8, relative to that of the parent duplex. Replacement of dG flanking the recognition site (XCGC/CGMG and GCGC/CGMX) led to decreases in the methylation rate by factors of 3.8 and 5, respectively. The v^{rel} value for the GCGCTC/CGMGAX duplex containing 8-oxoG two nucleotide residues from m5dC was 1.4 times lower than that of the GCGC/CGMG duplex. Thus, the presence of 8-oxoG suppresses DNA methylation by Dnmt3a-CD in most cases, and the magnitude of the effect depends on the position of the modified guanine residue.

The v^{rel} values for the unmethylated duplexes, XCGC/CGCG and GCXC/CGCG, were only 2- and 1.3-fold lower, respectively, than that of the parent duplex, GCGC/CGCG. The very low methylation rate of hemimethylated GCXC/CGMG suggests that Dnmt3a-CD preferably methylates the strand lacking 8-oxoG in the GCXC/CGCG duplex.

Binding of Dnmt3a-CD to 8-oxoG Duplexes. Changes in the methylation rates of 8-oxoG-containing duplexes may result from their altered binding affinity for Dnmt3a-CD. Therefore, binding measurements were performed in the presence of the cofactor analogue, AdoHcy, which facilitates formation of a specific complex between C5-MTases and DNA (*28, 29*) and prevents cytosine deamination (*30−32*). Complex formation was monitored using a fluorescence polarization technique with FAM-labeled oligodeoxynucleotides. The FAM label is unlikely to affect the stability of complexes of Dnmt3a-CD with 30-mer substrates, in view of earlier data showing no impact of FAM on the formation of 18-mer DNA−MTase complexes (*23*). Final polarization values were attained within 2 min and remained virtually constant (<10% decrease) over a further 90 min incubation period.

Binding curves for six duplexes are presented in Figure 2. The curves were nearly hyperbolic for the fGCGC/CGMG, fGCGC/CGMX, fGCGC/CXMG, and fGCGCTC/CGMGAX duplexes but clearly sigmoid for XCGC/CGMGf and GCXC/CGMGf, usually interpreted as evidence for positive binding cooperativity. Hill plots of binding data (inset of Figure 2) yielded Hill coefficients from 1.2 for fGCGC/CGMX and fGCGC/CXMG to 1.8 for XCGC/CGMGf and GCXC/CGMGf. However, this type of analysis has a serious limitation in our case, since it requires knowledge of the free, unbound Dnmt3a-CD concentration, which is significantly lower than the total concentration due to tight binding.

Several binding models were utilized to explain these data. A simple model implying a 1:1 binding stoichiometry and monomeric or dimeric Dnmt3a-CD as the binding unit showed marked systematic deviations with both fGCGC/CGMG and all 8-oxoG-containing duplexes and was consequently rejected. The quality of fit was not improved appreciably with models involving independent binding of two enzyme units (monomers of dimers) per duplex. A reasonably good fit was observed with the model shown in Scheme 1, which involves the successive binding of two enzyme units assumed to be Dnmt3a-CD homodimers. This theory is based on the structure of Dnmt3a-CD complexed

Table 2: Binding and Catalytic Properties of Oligodeoxynucleotide Duplexes in Reactions with Dnmt3a-CD and M.SssI

DNA duplex[a]	K_{d1} (nM)	K_{d2} (nM)	$K_{d1}K_{d2}$ (nM^2)	v^{rel} (%)[b]	k_{st} (h^{-1})	R (%)[c]	v^{rel} (%)[b]
			Dnmt3a-CD				M.SssI
GCGC CGMG	25 ± 8	33 ± 11	830	100	4.1 ± 0.3	30 ± 3	100
XCGC CGMG			14000 ± 4000	26 ± 5	3.0 ± 0.6	23 ± 4	140 ± 10
GCXC CGMG			9000 ± 1400	4 ± 2	3.1 ± 0.3	4 ± 1	< 0.4
GCGC CGMX	21 ± 3	13 ± 3	270	20 ± 2	2.2 ± 0.1	14 ± 2	130 ± 4
GCGC CXMG	11 ± 1	15 ± 1	165	180 ± 10	5.4 ± 0.6	31 ± 4	150 ± 30
GCGCTC CGMGAX	14 ± 1	12 ± 2	170	70 ± 10	3.0 ± 0.1	30 ± 5	90 ± 5
GMGC CGMG			2400 ± 250				
GCGC CGCG						60 ± 10	

[a] Oligodeoxynucleotide designations are as in Table 1. The target dC is underlined. The Dnmt3a-CD recognition site is in bold. [b] Relative rate of methylation. The rate for GCGC/CGMG (0.7 and 14 nM/min for Dnmt3a-CD and M.SssI, respectively) was taken to be 100%. [c] Fraction of DNA converted at the end of the reaction in Figure 3.
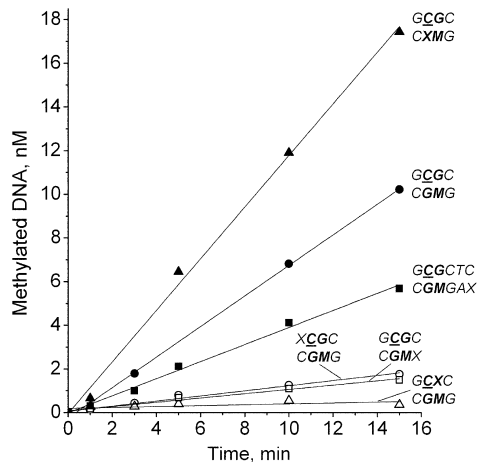

FIGURE 1: Time course of methylation of oligodeoxynucleotide duplexes by Dnmt3a-CD. The reaction mixtures contained 1.5 μM DNA, 0.88 μM Dnmt3a-CD, and 2 μM [CH$_3$-^{3}H]AdoMet: (●) GCGC/CGMG, (○) XCGC/CGMG, (△) GCXC/CGMG, (□) GCGC/CGMX, (▲) GCGC/CXMG, and (■) GCGCTC/CGMGAX.
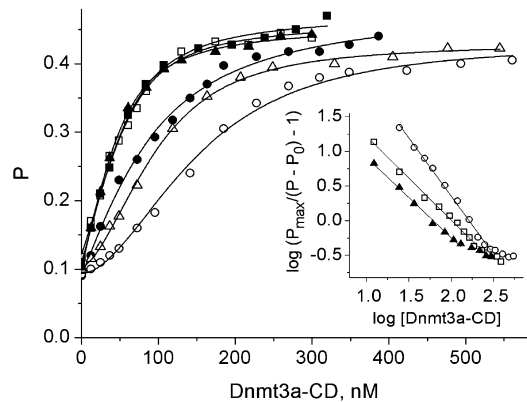

FIGURE 2: Binding curves obtained upon titration of fluorescein-labeled hemimethylated oligodeoxynucleotide duplexes (10 nM) with increasing amounts of Dnmt3a-CD in the presence of AdoHcy. P represents the polarization value. The lines signify the best fits of eqs 2−6. The inset is a Hill plot for three representative duplexes. Notations are as for Figure 1.

with its orthologous protein, Dnmt3L, gel filtration data presenting oligomerization of Dnmt3a-CD, and mutational analyses showing that dimeric Dnmt3a lacks catalytic activity (*33, 34*). Furthermore, the $P_{max} - P_0$ value, proportional to the volume of the bound protein, was 0.32−0.35 for Dnmt3a-CD complexes (Figure 2), compared with 0.09−0.11 for M.SssI complexed with fGCGC/CGMG (D. V. Maltseva and N. A. Cherepanova, unpublished results). As the molecular masses of Dnmt3a-CD and M.SssI are 36 and 44 kDa, respectively, the $P_{max} - P_0$ value is consistent with the binding of at least four Dnmt3a-CD monomers per duplex.

K_{d1} and K_{d2} values for all substrates were estimated by simultaneously fitting eqs 2−6 to the measured titration curves (listed in Table 2). For the XCGC/CGMGf and GCXC/CGMGf duplexes exhibiting sigmoid binding curves, only the product $K_{d1}K_{d2}$ could be estimated, since K_{d1} exceeded K_{d2} by at least 10-fold, rendering the ES complex stoichiometrically insignificant. In these cases (as well as for the doubly methylated duplex GMGC/CGMGf), estimates

of K_{d1} and K_{d2} were highly correlated and therefore unreliable. In contrast, the product $K_{d1}K_{d2}$ was estimated with good precision. The K_{d1} and K_{d2} values of fGCGC/CGMG and three duplexes containing the 8-oxoG lesion in the methylated strand (fGCGC/CGMX, fGCGC/CXMG, and fGCGCTC/CGMGAX) were similar. It appears that these substrates also exhibit apparent binding cooperativity, as the ratio of the macroscopic constants (K_{d2}/K_{d1}) should be 4 for independent binding to two sites with identical microscopic constants (*35*). Notably, methylation of the second strand in the GCGC/CGMGf duplex devoid of 8-oxoG to form fully methylated GMGC/CGMGf duplex was sufficient to decrease K_{d2}/K_{d1} to <5, thus making binding highly cooperative. The product $K_{d1}K_{d2}$ was markedly increased, compared with that of the hemimethylated counterpart, as expected (Table 2).

As specified in Table 2, introduction of 8-oxoG leads to a minor reduction in K_{d1} and K_{d2}, with a concomitant 3−5-fold decrease in $K_{d1}K_{d2}$, unless the lesion is 5′ adjacent to or within the CpG site, 3′ from the target cytosine. In the latter case, $K_{d1}K_{d2}$ is markedly increased (by 11−17-fold), presumably due to the increased K_{d1} (as estimated from the higher
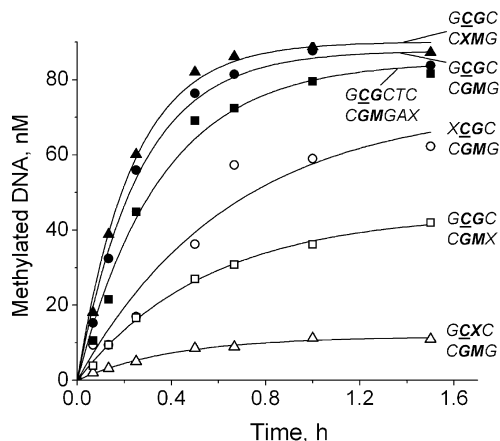
FIGURE 3: Complete time course of methylation of hemimethylated oligodeoxynucleotide duplexes by Dnmt3a-CD. The reaction mixtures contained 0.3 μM DNA, 3 μM Dnmt3a-CD, and 1.2 μM [CH$_3$-^{3}H]AdoMet. The lines signify the best fits of eq 1. Notations are as for Figure 1.
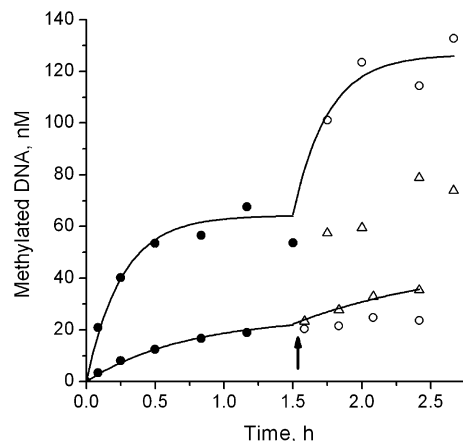

FIGURE 4: Effects of the repeated addition of Dnmt3a-CD and GCGC/CGMG on the time course of methylation. The reaction mixture initially contained 0.3 μM GCGC/CGMG and 3 μM Dnmt3a-CD (top curve) or 0.94 μM GCGC/CGMG and 0.3 μM Dnmt3a-CD (bottom curve). The [CH$_3$-^{3}H]AdoMet concentration used was 1.2 μM. At the time point indicated with an arrow, fresh Dnmt3a-CD ($\triangle$) or GCGC/CGMG ($\bigcirc$) was added to double its total concentration in the assay medium.

K_{d1}/K_{d2} ratio), disallowing separate estimation of the binding constants. Thus, 8-oxoG affects the stability of the complete enzyme−substrate complex, and the magnitude of the effect depends on the position of the lesion relative to the target cytosine. Notably, data fits assuming monomeric Dnmt3a as the binding unit in Scheme 1 yielded K_{d1} and K_{d2} values that were 2−3 times larger but did not influence our conclusions.

Integral Kinetics of Methylation. Informative results were obtained from analysis of the complete time course of the methylation reaction. The reaction was performed with a 10-fold excess of Dnmt3a-CD over duplex substrate. The Dnmt3a-CD concentration used (3 μM), based on Figure 2, was nearly saturating, allowing conversion of the majority of the duplex to a complex with Dnmt3a-CD. The time course of the reaction (Figure 3) was described by a simple exponential function (eq 1), yielding relatively consistent k_{st} values differing by a factor of 2 (Table 2). Importantly, the final yield of the [CH$_3$-^{3}H]DNA product, R, depended on the duplex used but was significantly lower than the expected value of 100% in all cases (Figure 3). The final yield was only 30%, even with the hemimethylated substrate GCGC/CGMG lacking 8-oxoG. The product yield correlated well with the v^{rel} value (Table 2), and both parameters were lowest with GCXC/CGMG.

The results of the following control experiments ruled out the trivial explanation of incomplete substrate conversion due to nonspecific inactivation of the enzyme or substrate during catalysis. First, addition of fresh enzyme after the amount of product leveled off did not stimulate further methylation, whereas addition of fresh substrate led to similar product formation (Figure 4). These results indicated that substrate was the limiting factor under these conditions. Second, a comparable low product yield was observed when the reaction was performed with excess substrate over enzyme, but the effects of fresh enzyme and substrate were reversed in this case (Figure 4), pointing to enzyme as the limiting factor. Moreover, the final product yield was only 7% of the initial enzyme concentration. The results of this section collectively indicate that, besides forming productive complex with its oligodeoxynucleotide duplex substrates, Dnmt3a-CD forms tight, slowly dissociating nonproductive com-

plexes. The presence of 8-oxoG in certain positions appears to increase the probability of this aberrant reaction, as indicated by decreased R values (Table 2). This finding is consistent with the results obtained from surface plasmon resonance experiments showing very slow DNA release from enzyme−DNA complexes (*36*). The invariance of k_{st} values implies that once formed, productive enzyme−substrate complexes undergo methylation with a rate constant that is virtually independent of 8-oxoG and its occupied position.

An alternative explanation for incomplete substrate conversion is that the enzyme preparation contains inactive enzyme that still retains the ability to bind DNA tightly. However, this theory is inconsistent with the observation that the R value varies considerably, depending on the substrate used. Furthermore, SDS−PAGE analysis revealed no heterogeneity in the Dnmt3a-CD preparation.

Methylation Kinetics of M.SssI. The substrate specificity of the prokaryotic DNA methyltransferase, SssI, is identical to that of Dnmt3a (*37*). We measured only the initial rates of methylation of six hemimethylated duplexes by M.SssI, as described above for Dnmt3a-CD. The time courses were linear, generating v^{rel} values listed in Table 2. This enzyme was even more specific with respect to the 8-oxoG position. The GCXC/CGMG duplex containing the 8-oxoG lesion in the recognition site was not methylated at all (Table 2), while either no effect or stimulation of the methylation reaction by a factor of 1.3−1.5 was observed with duplexes containing the 8-oxoG lesion at other positions.

DISCUSSION

In this study, we examined the effects of the 8-oxoG lesion on the functional properties of the catalytic domain of murine Dnmt3a. In view of the finding that Dnmt3a can methylate both DNA strands, we mainly employed hemimethylated oligodeoxynucleotide duplexes as substrates, which allowed us to examine the effects of 8-oxoG on methylation of a particular DNA strand.

The presence of 8-oxoG in most hemimethylated duplexes decreased the initial rates of methylation by Dnmt3a-CD.

The most significant effect was observed when 8-oxoG replaced G within the CpG recognition site [GCXC/CGMG (Table 2)]. The location of 8-oxoG adjacent to the recognition site on the 5′-side in XCGC/CGMG and GCGC/CGMX also slowed methylation, but to a lesser extent. When positioned opposite the target C, the 8-oxoG lesion markedly accelerated the methylation reaction. Thus, we propose that the impact of the 8-oxoG lesion on DNA methylation by Dnmt3a-CD depends on the location of the damaged guanine relative to the DNA recognition site of the enzyme.

MTase SssI exhibited even greater positional specificity, as it did not methylate substrates with the modified recognition site but showed similar or even enhanced activity with other modified substrates (Table 2). Similar results have been reported for human MTase Dnmt1 and prokaryotic MTase HpaII (*21, 22*), which exhibited the largest reduction in methylation rate when 8-oxoG replaced guanine within the recognition sites 3′ from the target cytosine. Dnmt3a-CD is also similar to Dnmt1 in that the presence of 8-oxoG in one strand does not prevent methylation of the other strand. In contrast, methylation of the target CCGG site in both strands by M.HpaII is prevented by the presence of a single 8-oxoG in one strand.

The impact of introducing 8-oxoG on oligodeoxynucleotide duplex binding measured using the fluorescence polarization technique correlated reasonably well with its effects on the initial rate of methylation. The binding profiles indicate the existence of two types of binding sites with similar affinities for Dnmt3a-CD in duplexes containing either no 8-oxoG (GCGC/CGMG) or 8-oxoG only in the methylated strand (GCGC/CXMG, GCGC/CGMX, and GCGCTC/CGMGAX). With all three duplexes (XCGC/CGMG, GCXC/CGMG, and GCGC/CGMX) displaying a marked decrease in ν^{rel}, the binding affinity of the site that interacts initially is lower than that of the second binding site ($K_{d1} > K_{d2}$). This behavior may result from ordered binding to two adjacent sites such that the first bound Dnmt3a-CD dimer comprises part of the binding site for the second dimer. Recent X-ray crystallographic data on the Dnmt3a−Dnmt3L complex (*33*) are consistent with this interpretation. The results suggest that DNA binds two Dnmt3a-CD−Dnmt3L pairs, with the two active sites ∼40 Å apart. According to this model, Dnmt3a methylates two CpGs separated by one helical turn. DNA contacts each pair through the Dnmt3a active site but has no contact with Dnmt3L. For our 30-mer substrates, one Dnmt3a-CD−Dnmt3L pair should be at the CpG recognition site and the other pair at a nonspecific sequence. As Dnmt3L is a close ortholog of Dnmt3a, we suggest that both bound Dnmt3a dimers mimic the Dnmt3a−Dnmt3L pairs and interact with DNA in a similar manner through one of the two active sites present in the dimer. The first binding event is likely to involve the recognition site. The second Dnmt3a dimer interacts less specifically with DNA, but its binding is supported by interactions with the bound dimer. In terms of this mechanism, 8-oxoG located at or close to the recognition site weakens binding of the first dimer (increases K_{d1}) but has no effect on K_{d2}, thereby increasing $K_{d1}K_{d2}$ and the sigmoidicity of the binding curve. Alternatively, multimerization of the proteins on DNA may require conformational changes in DNA. Interference of 8-oxoG with such

alterations may explain the increased cooperativity of binding to 8-oxoG-modified DNA.

However, the effects of 8-oxoG on DNA binding affinity could not simply justify its impact on the methylation rate. Despite variations in binding affinity, the concentration of the duplexes used for Figure 1 was nearly saturating in all cases (Figure 2). Analysis of the complete time course of the methylation reaction was particularly helpful, as the data showed that Dnmt3a-CD can form tight nonproductive complexes with its substrates. Even with the normal hemimethylated substrate, GCGC/CGMG, only 30% of the enzyme−substrate complex is productive, as characterized by the R value (Table 2). This percentage was further decreased with duplexes displaying the lowest ν^{rel} values, thus explaining the effect of 8-oxoG on ν^{rel}.

The effects of 8-oxoG on binding affinity and R appear closely related. Nonproductive complexes may largely result from Dnmt3a-CD binding to the methylated strand. This theory is supported by the ability of the fully methylated duplex to bind Dnmt3a-CD (Table 2). Moreover, the R value increased to 60% with the unmethylated duplex (Table 2). An R value of 90% was observed with the unmethylated 18-mer duplex, 5′-GAGCCAAGCGCACTCTGA/CTCG-GTTCGCGTGAGACT-5′, indicating no nonproductive binding, and 30% with the hemimethylated form (V. B. Baskunov and E. S. Gromova, unpublished results). Under these conditions, weakening of Dnmt3a-CD binding to the target strand by 8-oxoG would clearly enhance the probability of nonproductive binding to the other strand. Each hemimethylated DNA may therefore bind Dnmt3a-CD either productively or nonproductively. The proportion of each binding type will depend on the relative affinities of the corresponding binding sites and possibly rates of binding, as the resulting complexes seem to dissociate very slowly and no redistribution of Dnmt3a-CD occurs on the time scale of methylation. An important inference is that the binding constants derived from fluorescence polarization measurements represent combinations of the binding constants for productive and nonproductive binding and may even be not true equilibrium constants if a kinetic factor is involved.

The molecular basis for the effects of 8-oxoG on interactions of DNA with Dmnt3a remains to be determined. Molecular dynamics, NMR, and X-ray crystallographic analyses disclose that the introduction of 8-oxoG into DNA results in small changes in the phosphodiester group conformation and a helical twist near the damaged guanine but induces no significant alterations in the DNA B-form structure (*6−8*). A distinctive feature of 8-oxoG is an altered pattern of potential hydrogen bonding in comparison with guanine: a hydrogen atom added to N7 converts it from a proton acceptor to donor, and a strong hydrogen bond acceptor, an oxygen atom, appears at C8 (Figure 5). This may lead to changes in the hydrogen bond network linking the enzyme and DNA, modulating the stability of the complex and hence the probability of nonproductive binding. Notably, M.SssI forms direct contacts with N7 (*38, 39*). M.SssI is another C5 MTase that also recognizes the CpG site, shares conserved active site sequence motifs with Dnmt3a, and displays similar sensitivity to 8-oxoG. It would be of interest to determine whether the mechanism underlying the effect of 8-oxoG on M.SssI is analogous to that established for Dnmt3a. Another attractive target is human
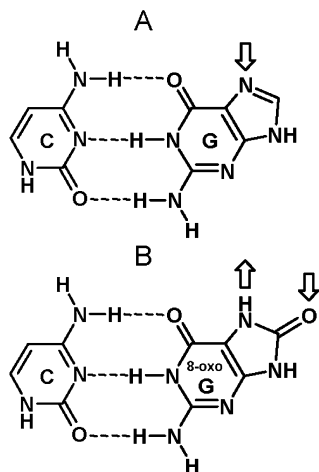
FIGURE 5: Normal C-G (A) and C-8-oxoG (B) base pairs. Changed hydrogen bond acceptors and donors are indicated by arrows directed toward and away from the base pair, respectively.

topoisomerase I, in which stabilization of the protein−(8-oxoG-damaged DNA) complex in an inactive conformation has recently been reported (*12*).

While the 8-oxoG lesion does not interfere with methylation of unmethylated DNA by Dnmt3a (the first step of *de novo* methylation), methylation of hemimethylated DNA (the second step of *de novo* methylation) is severely affected. In cells, methylation of hemimethylated DNA is accomplished by Dnmt1, a maintenance MTase (*18, 40*). However, the ability of Dnmt1 to methylate the target cytosine when 8-oxoG is placed within the CpG sites 3′ from the target cytosine is also strongly diminished (*21*). Hence, introduction of 8-oxoG lesions into DNA leads to potential alterations in *de novo* methylation.

In summary, our data suggest that the 8-oxoG damage at or close to the recognition site weakens the affinity of hemimethylated DNA for Dnmt3a, thereby favoring nonproductive binding and slowing methylation of the second strand.

ACKNOWLEDGMENT

REFERENCES

1. Lindahl, T., and Wood, R. D. (1999) Quality control by DNA repair. *Science 286*, 1897–1905.
2. Cooke, M. S., Evans, M. D., Dizdaroglu, M., and Lunec, J. (2003) Oxidative DNA damage: Mechanisms, mutation and disease. *FASEB J. 17*, 1195–1214.
3. Valko, M., Izakovic, M., Mazur, M., Rhodes, C. J., and Telser, J. (2004) Role of radicals in DNA damage and cancer incidence. *Mol. Cell. Biochem. 266*, 37–56.
4. Greenberg, M. M. (2004) In vitro and in vivo effects of oxidative damage to deoxyguanosine. *Biochem. Soc. Trans. 32*, 46–50.
5. Marnett, L. J., Riggins, J. N., and West, J. D. (2003) Endogenous generation of reactive oxidants and electrophiles and their reactions with DNA and protein. *J. Clin. Invest. 111*, 583–593.
6. Ishida, H. (2002) Molecular dynamic simulation of 7,8-dihydro-8-oxoguanine DNA. *J. Biomol. Struct. Dyn. 19*, 839–851.
7. Lipscomb, L. A., Peek, M. E., Morningstar, M. L., Verghis, S. M., Miller, E. M., Rich, A., Essigmann, J. M., and Williams, L. D. (1995) X-ray structure of a DNA decamer containing 7,8-dihydro-8-oxoguanine. *Proc. Natl. Acad. Sci. U.S.A. 92*, 719–723.

8. Oda, Y., Uesugi, S., Ikehara, M., Nishimura, S., Kawase, Y., Ishikawa, H., Inoue, H., and Ohtsuka, E. (1991) NMR studies of a DNA containing 8-hydroxydeoxyguanosine. *Nucleic Acids Res. 19*, 1407–1412.
9. Lukin, M., and de los Santos, C. (2006) NMR structures of damaged DNA. *Chem. Rev. 106*, 607–689.
10. Valko, M., Rhodes, C. J., Moncol, J., Izakovic, M., and Mazur, M. (2006) Free radicals, metals and antioxidants in oxidative stress-induced cancer. *Chem.-Biol. Interact. 160*, 1–40.
11. Pourquier, P., Ueng, L.-M., Fertala, J., Wang, D., Park, H.-J., Essigmann, J. M., Bjornsti, M.-A., and Pommier, Y. (1999) Induction of reversible complex between eukaryotic DNA topoisomerase I and DNA-containing oxidative base damages. *J. Biol. Chem. 274*, 8516–8523.
12. Lesher, D. T., Pommier, Y., Stewart, L., and Redinbo, M. R. (2002) 8-Oxoguanine rearranges the active site of human topoisomerase I. *Proc. Natl. Acad. Sci. U.S.A. 99*, 12102–12107.
13. Ghosh, R., and Mitchell, D. L. (1999) Effect of oxidative DNA damage in promoter elements on transcription factor binding. *Nucleic Acids Res. 27*, 3213–3218.
14. Ramon, O., Sauvaigo, S., Gasparutto, D., Faure, P., Favier, A., and Cadet, J. (1999) Effects of 8-oxo-7,8-dihydro-2′-deoxyguanosine on the binding of the transcription factor Sp1 to its cognate target DNA sequence (GC box). *Free Radical Res. 31*, 217–229.
15. Valinluck, V., Tsai, H.-H., Rogstad, D. K., Burdzy, A., Bird, A., and Sowers, L. C. (2004) Oxidative damage to methyl-CpG sequences inhibits the binding of the methyl-CpG binding domain (MBD) of methyl-CpG binding protein 2 (MeCP2). *Nucleic Acids Res. 32*, 4100–4108.
16. Cerda, S., and Weitzman, S. A. (1997) Influence of oxygen radical injury on DNA methylation. *Mutat. Res. 386*, 141–152.
17. Hermann, A., Gowher, H., and Jeltsch, A. (2004) Biochemistry and biology of mammalian DNA methyltransferases. *Cell. Mol. Life Sci. 61*, 2571–2587.
18. Jeltsch, A. (2006) Molecular enzymology of mammalian DNA methyltransferases. *Curr. Top. Microbiol. Immunol. 301*, 203–225.
19. Jirtle, R. L., and Skinner, M. K. (2007) Environmental epigenomics and disease susceptibily. *Nat. Rev. Genet. 8*, 253–262.
20. Esteller, M. (2007) Cancer epigenomics: DNA methylomes and histone-modification maps. *Nat. Rev. Genet. 8*, 286–298.
21. Turk, P. W., Laayoun, A., Smith, S. S., and Weitzman, S. A. (1995) DNA adduct 8-hydroxyl-2′-deoxyguanosine (8-hydroxyguanine) affects function of human DNA methyltransferase. *Carcinogenesis 16*, 1253–1255.
22. Weitzman, S. A., Turk, P. W., Milkowski, D. H., and Kozlowski, K. (1994) Free radical adducts induce alterations in DNA cytosine methylation. *Proc. Natl. Acad. Sci. U.S.A. 91*, 1261–1264.
23. Baskunov, V. B., Subach, F. V., Kolbanovskiy, A., Kolbanovskiy, M., Eremin, S., Johnson, F., Bonala, R., Geacintov, N. E., and Gromova, E. S. (2005) Effects of benzo[*a*]pyrene-deoxyguanosine lesions on DNA methylation catalyzed by EcoRII DNA methyltransferase and on DNA cleavage effected by EcoRII restriction endonuclease. *Biochemistry 44*, 1054–1066.
24. Gowher, H., and Jeltsch, A. (2001) Enzymatic properties of recombinant Dnmt3a DNA methyltransferases from mouse: The enzyme modifies DNA in a non-processive manner and also methylates non-CpG sites. *J. Mol. Biol. 309*, 1201–1208.
25. Darii, M. V., Kirsanova, O. V., Drutsa, V. L., Kochetkov, S. N., and Gromova, E. S. (2007) Purification and site-directed mutagenesis of DNA methyltransferase SssI. *Mol. Biol. (Moscow) 41*, 121–129.
26. Brennan, C. A., Van Cleve, M. D., and Gumport, R. I. (1986) The effects of base analogue substitutions on the methylation by the EcoRI modification methylase of octadeoxyribonucleotides containing modified EcoRI recognition sequences. *J. Biol. Chem. 261*, 7279–7286.
27. Subach, O. M., Khoroshaev, A. V., Gerasimov, D. N., Baskunov, V. B., Shchyolkina, A. K., and Gromova, E. S. (2004) 2-Pyrimidinone as a probe for studying the EcoRII DNA methyltransferase-substrate interaction. *Eur. J. Biochem. 271*, 2391–2399.
28. Wyszynski, M. W., Gabbara, S., Kubareva, E. A., Romanova, E. A., Oretskaya, T. S., Gromova, E. S., Shabarova, Z. A., and Bhagwat, A. S. (1993) The cysteine conserved among DNA cytosine methylases is required for methyl transfer, but not for specific DNA binding. *Nucleic Acids Res. 21*, 295–301.
29. Klimasauskas, S., and Roberts, R. J. (1995) M.HhaI binds tightly to substrates containing mismatches at the target base. *Nucleic Acids Res. 23*, 1388–1395.

30. Zingg, J.-M., Shen, J.-C., Yang, A. S., Rapoport, H., and Jones, P. A. (1996) Methyalation inhibitors can increase the rate of cytosine deamination by (cytosine-5)-DNA methyltransferase. *Nucleic Acids Res. 24*, 3267–3275.

31. Shen, J. C., III, and Jones, P. A. (1992) High frequency mutagenesis by a DNA methyltransferase. *Cell 71*, 1073–1080.

32. Wyszynski, M., Gabbara, S., and Bhagwat, A. S. (1994) Cytosine deaminations catalyzed by DNA cytosine methyltransferases are unlikely to be the major cause of mutational hot spots at sites of cytosine methylation in *Escherichia coli*. *Proc. Natl. Acad. Sci. U.S.A. 91*, 1574–1578.

33. Jia, D., Jurkowska, R. Z., Zhang, X., Jeltsch, A., and Cheng, X. (2007) Structure of Dnmt3a bound to Dnmt3L suggests a model for *de novo* DNA methylation. *Nature 449*, 248–251.

34. Cheng, X., and Blumenthal, R. (2008) Mammalian DNA methyltransferases: A structural perspective. *Structure 16*, 341–350.

35. Dixon, M., Webb, E. C., Thorne, C. J. R., and Tipton, K. F. (1979) *Enzymes*, 3rd ed., pp 140−148, Longman Group Ltd., London.

36. Gowher, H., Liebert, K., Hermann, A., Xu, G., and Jeltsch, A. (2005) Mechanism of stimulation of catalytic activity of Dnmt3a and Dnmt3b DNA-(cytosine-C5)-methyltransferases by Dnmt3L. *J. Biol. Chem. 280*, 13341–13348.

37. Nur, I., Szyf, M., Razin, A., Glaser, G., Rottem, S., and Razin, S. (1985) Procaryotic and eucaryotic traits of DNA methylation in spiroplasmas (mycoplasmas). *J. Bacteriol. 164*, 19–24.

38. Koudan, E. V., Bujnicki, J. M., and Gromova, E. S. (2004) Homology modeling of the CG-specific DNA methyltransferase SssI and its complexes with DNA and AdoHcy. *J. Biomol. Struct. Dyn. 22*, 339–345.

39. Renbaum, P., and Razin, A. (1995) Footprint analysis of M.SssI and M.HhaI methyltransferases reveals extensive interactions with the substrate DNA backbone. *J. Mol. Biol. 248*, 19–26.

40. Fatemi, M., Hermann, A., Gowher, H., and Jeltsch, A. (2002) Dnmt3a and Dnmt1 functionally cooperate during methylation of DNA. *Eur. J. Biochem. 269*, 4981–4984.